

High strength bioactive glass-ceramic scaffolds for bone regeneration

Original

High strength bioactive glass-ceramic scaffolds for bone regeneration / VITALE BROVARONE, Chiara; BAINO, Francesco; VERNE', ENRICA. - In: JOURNAL OF MATERIALS SCIENCE. MATERIALS IN MEDICINE. - ISSN 0957-4530. - STAMPA. - 20:(2009), pp. 643-653. [10.1007/s10856-008-3605-0]

Availability:

This version is available at: 11583/1847272 since:

Publisher:

Springer

Published

DOI:10.1007/s10856-008-3605-0

Terms of use:

This article is made available under terms and conditions as specified in the corresponding bibliographic description in the repository

Publisher copyright

(Article begins on next page)

High strength bioactive glass-ceramic scaffolds for bone regeneration

Chiara Vitale-Brovarone, Francesco Baino, Enrica Verné*

This is the author post-print version of an article published on *Journal of Materials Science: Materials in Medicine*, Vol. 20, pp. 643-653, 2009 (ISSN 0957-4530).

The final publication is available at

<http://link.springer.com/article/10.1007%2Fs10856-008-3605-0>.

This version does not contain journal formatting and may contain minor changes with respect to the published edition.

The present version is accessible on PORTO, the Open Access Repository of the Politecnico of Torino, in compliance with the publisher's copyright policy.

Copyright owner: *Springer*.

Materials Science and Chemical Engineering Department, Politecnico di Torino, Italy

*Corresponding author: Enrica Verné

Tel.: +39 011 5644717

Fax: + 39 011 5644699

E-mail address: enrica.verne@polito.it

Abstract

This research work is focused on the preparation of macroporous glass-ceramic scaffolds with high mechanical strength, equivalent with cancellous bone. The scaffolds were prepared using an open-cells polyurethane sponge as a template and glass powders belonging to the system $\text{SiO}_2\text{-P}_2\text{O}_5\text{-CaO-MgO-Na}_2\text{O-K}_2\text{O}$. The glass, named as CEL2, was synthesized by a conventional melting-quenching route, ground and sieved to obtain powders of specific size. A slurry of CEL2 powders, polyvinyl alcohol (PVA) as a binder and water was prepared in order to coat, by a process of impregnation, the polymeric template. A thermal treatment was then used to remove the sponge and to sinter the glass powders, in order to obtain a replica of the template structure. The scaffolds were characterized by means of X-ray diffraction analysis, morphological observations, density measurements, volumetric shrinkage, image analysis, capillarity tests, mechanical tests and *in vitro* bioactivity evaluation.

Keywords: Glass-ceramic; Scaffold; High mechanical strength; Bone grafting.

1 Introduction

Since the birth of orthopaedic surgery, bone losses were traditionally replaced by using materials coming from the patient body (autograft) or from an external donor (allograft). Autografts are generally considered the more effective solution for bone replacing and substitution, but the bone volume that can be safely drawn is limited and problems of pain or morbidity in the harvest site can occur for the patient [1]. The use of allografts, although stored in proper bone banks, could involve the risk of pathogen diseases transfer from the donor to the patient and besides their quality can be not always satisfactory [2]. Thus, an increasing interest has been turned to synthetic materials, that overcome antigenicity and morbidity problems, are available without amount limitations and can be easily processed to obtain scaffolds [3]. Bioceramics have been widely investigated as bone graft materials for many decades, and have a range of applications including bone defects filling [4], fracture fixation [5], trauma [6], tumors [7], maxillofacial [8] and spinal surgery [9], drug delivery systems [10]. Among the glass and ceramic materials, calcium and phosphate salts [11], calcium sulfate [5], hydroxyapatite (HAp) [12], bioactive glasses and glass-ceramics [13,14] are usually used for scaffolds preparation.

An effective scaffold for bone tissue engineering should promote bone regeneration. At this purpose, a network of open and highly interconnected macropores in the 100-500 μm range is required in order to allow the vascularization of the scaffold [15].

Microporosity is another important feature because it favours proteins adhesion and thus cells attachment on the scaffold and allows the flow of nutrients to reach the cells within the scaffold [16]. The scaffold roughness is also a crucial point for the implant success, because it is known that a rough surface stimulates osteoblasts adhesion and proliferation [17].

A good balance between a high degree of porosity and mechanical properties comparable with cancellous bone (2-12 MPa) must be pursued [18]. Previous investigations demonstrated that it is not easy to reach this compromise: in many studies ceramic scaffolds with a very good degree of

porosity (above 50 %vol. is usually required) but unsatisfactory mechanical properties (below 1 MPa) were produced [19,20]. A scaffold for bone substitution should be bioactive, *i.e.* the implant is not only osteoinductive, but also induces osteoproduction [21,22]. Bioactive scaffolds can favour the apposition of new bone on their surfaces through a complex mechanism of ion exchange with body fluids and stimulate the differentiation and maturation of mesenchimal stem cells into osteoblasts [23].

Glass and glass-ceramic scaffolds can be prepared by using different methods; for instance, freeform fabrication techniques [24], sponge replication [25,26], starch consolidation [27] and polymeric particles burning-out [28].

The sponge replication method was chosen for the present work. A commercial polyurethane sponge, possessing an open and interconnected structure, was used as a template for a ceramic replica through its impregnation with a slurry of glass powders followed by a thermal treatment. This work is focused on the preparation and characterizations of glass-ceramic bioactive scaffolds with trabecular texture and mechanical properties analogous to cancellous bone. Specifically, the aim of this research concerns the optimisation of the scaffold mechanical properties in order to improve the results obtained in a previous work, in which scaffolds possessing a mechanical strength of 1.0 ± 0.4 MPa were described [25]. The main effort was spent in order to set up a processing schedule able to lead to a bioactive glass-ceramic scaffold with tailored porosity, according to the above mentioned requirement for a bone scaffold, without compositional modifications of the glass.

2 Experimental procedure

2.1 Materials

In this research work, glass-ceramic macroporous scaffolds were prepared using a polyurethane sponge as organic template and bioactive glass-ceramic powders.

The chosen glass-ceramic, hereafter named as CEL2 [29], belongs to the system $\text{SiO}_2\text{-P}_2\text{O}_5\text{-CaO-MgO-Na}_2\text{O-K}_2\text{O}$ and has the following molar composition: 45% SiO_2 , 3% P_2O_5 , 26% CaO , 7% MgO , 15% Na_2O , 4% K_2O .

Briefly, CEL2 was prepared by melting the raw products (SiO_2 , $\text{Ca}_3(\text{PO}_4)_2$, CaCO_3 , $4\text{MgCO}_3\text{Mg}(\text{OH})_2\cdot 5\text{H}_2\text{O}$, Na_2CO_3 , K_2CO_3) in a platinum crucible at 1400 °C for 1 h in air and by then quenching the melt in cold water to obtain a frit, that was subsequently ground by ball milling and sieved to a final grain size below 30 μm . The glass CEL2 was thermally characterized in a previous work [29] and showed a glass transition temperature T_g at 550 °C and two crystallization temperature T_{X1} at 600 °C and T_{X2} at 800 °C.

2.2 Scaffolds preparation

The chosen organic template is a commercial polyurethane sponge with an open and interconnected macroporosity. The sponge was cut into 1.5 cm \times 1.5 cm \times 1.5 cm cubic blocks, and then impregnated with a water-based CEL2 slurry.

CEL2 slurry was prepared by dispersing the glass powders into distilled water with polyvinyl alcohol (PVA) used as binder in order to control the slurry viscosity and to optimise the ability of glass particles to uniformly coat the sponge. The weight ratio of the slurry components was: 30% CEL2, 6% PVA, 64% water (final solid load 30% wt.). First PVA was hydrolyzed and stirred in distilled water at a temperature of 60 °C for 1 h, and then CEL2 powders were dispersed in the solution. The water evaporated during PVA dissolution was re-added in order to obtain the chosen solid load. Then the porous sponge underwent the impregnation process. The sponge blocks were soaked into the glass slurry for 60 s and taken back for several times, followed by cycles of

compression to reduce the sponge in thickness along the three spatial directions, in order to remove the exceeding slurry. In particular, the sponge blocks underwent a pressure of 20 kPa for 1 s.

In this work, different impregnation processes, labelled as method A, B and C, were carried out in order to optimise the mechanical strength of the scaffolds through a better covering of the polymeric template.

The features of the three methods can be resumed as it follows:

- method A: the sponge blocks were soaked in the CEL2 slurry and shrunk up to 60% in thickness along the three spatial directions; these impregnation/compression cycles were repeated for three times. After each cycle the impregnated sponge was left 60 s in air to restore and de-compress.
- method B: the sponge blocks were soaked in the CEL2 slurry and shrunk up to 60% in thickness along the three spatial directions; this infiltration/compression cycle was repeated for three times. A further cycle in which the sponge was shrunk only up to 33% in thickness, was added. Also in this case the cycles are spaced by 60 s of restore.
- method C: the sponge blocks were soaked in the CEL2 slurry and shrunk up to 60% in thickness along the three spatial directions; this infiltration/compression cycle was repeated for three times. A further cycle of impregnation without any compression was added. Also in this case the cycles are spaced by 60 s of restore.

After the impregnation phase, the samples were dried at room temperature for 3 h and then introduced into the furnace at room temperature. The thermal treatment was performed at 950 °C (method A and B) or at 1000 °C (method C) for 3 h (heating and cooling rate were 5 and 10 °C/min respectively) in order to remove the organic phase and to sinter the inorganic one, obtaining macroporous glass-ceramic scaffolds.

In addition another three sub-methods of preparation, labelled from now on as A-1, B-1 and B-2, were performed in order to optimise step-by-step the mechanical properties maintaining a

satisfactory degree of porosity. The impregnation process of method A-1 was the same of method A, but before sintering at 950 °C for 3 h the samples underwent a two-steps drying process: thermal treatment at 80 °C for 2 h (heating rate 3 °C/min) in order to gradually evaporate the ethanol followed by a treatment at 600 °C for 2 h (heating rate 3 °C/min) to remove the polymeric sponge at a constant temperature. This procedure was set in order to avoid the formation of cracks in the impregnated body and during the skeleton removal.

The method B-1 involved the use, in the starting slurry, of ethylene glycol (EG) as drying chemical control additive (DCCA). Specifically, the weight ratio of the slurry components was modified as follows: 30% CEL2, 6% PVA, 10% EG, 54% water. The presence of EG, as previously reported in literature, should lead to the prevention of cracks formation during the drying process of the samples [11,30] and thus obtaining an increase of the mechanical properties.

In the method B-2 the sponge impregnation was the same of method B, but the thermal treatment was set at 1000 °C for 3 h in order to investigate the influence of the degree of sintering on the final mechanical strength.

Details of the methods adopted for the scaffold preparation are summarized in table 1.

2.3 Scaffolds characterization

X-ray diffraction (X'Pert Philips diffractometer) using the Bragg Brentano camera geometry and the Cu-K α incident radiation, was carried out on the scaffolds reduced into powders in order to assess the presence of crystalline phases. The microstructure of the scaffolds was qualitatively studied through scanning electron microscopy (SEM Philips 525 M) in order to observe the degree of sintering (presence of dense sintering necks) and to evaluate the pores size, morphology, distribution and interconnection.

The total pore content (% vol.) of the scaffolds was assessed through weight measurements testing five polished 1 cm × 1 cm × 1 cm samples, prepared according to each methods reported in table 1, by the following calculation:

$$\left(1 - \frac{W_m}{W_{th}}\right) \times 100$$

where W_m is the measured weight and W_{th} the theoretical one calculated from the product of glass density and the sample volume.

The presence of a highly interconnected pores network and a diffuse microporosity was qualitatively assessed through capillarity tests using bovine serum, in which some drops of red ink were dispersed, to simulate the colour of biological fluids. A face of the scaffold was put into contact with a thin film of fluid, to verify if serum was infiltrating the scaffold due to capillarity forces.

In addition, a quantitative evaluation of the pores size distribution and amount was attained through image analysis studies (Qwin Leica software) on different scaffold cross-sections. The volumetric shrinkage of the impregnated sponges, due to the organic skeleton removal and to the CEL2 softening and sintering, was evaluated by measuring five samples for each type of the prepared scaffolds as $\left(1 - \frac{V_s}{V_0}\right) \times 100$, where V_s is the scaffold volume and V_0 is the volume of the impregnated sponge before the thermal treatment.

The scaffolds were carefully polished to obtain 1 cm × 1 cm × 1 cm cubic samples used for the mechanical tests. The strength of the scaffolds was evaluated through destructive compressive tests using an Instron machine and testing 5 specimens for each preparation method. The failure stress was obtained dividing the maximum load registered during the test by the resistant section area; the cross-head speed was 1 mm/min.

The bioactivity study was carried out *in vitro* by soaking the scaffolds for 1 week in a simulated body fluid (SBF), which has an ions concentrations analogous to human plasma [31]. Specifically,

cubic samples were soaked in 30 ml of SBF maintained at 37 °C in polyethylene bottles; every 48 h a refresh of the solution was carried out to simulate fluid circulation in the human body.

3 Results and discussion

Figure 1 shows the morphology of the polyurethane open-cells sponge used as a template for the preparation of CEL2 glass-ceramic scaffolds. The sponge has a 3-D highly interconnected structure analogous to cancellous bone. Pores size ranged from 100 up to 1000 µm and the thickness of the trabeculae is few tens of microns. The choice of CEL2 as starting material for the scaffolds was due to its excellent biological behaviour, as already assessed in a previous work [25].

The polymeric sponge can be easily cut, thus, as shown in figure 2, scaffolds of various shapes – cubic, prismatic, thin regular plate – can be produced.

The impregnation process and the drying conditions of the impregnated sponge were optimised in order to enhance the mechanical strength of the scaffolds maintaining a satisfactory porosity degree. The scaffolds were obtained through a thermal treatment at 950 °C or 1000 °C for 3 h. The polyurethane sponge was completely removed at 600 °C, thus no contamination of the scaffolds was foreseen and actually assessed.

The scaffolds were characterized by means of XRD analysis, morphological observations (SEM), *in vitro* and biological tests, volumetric shrinkage, density measurements, image analysis, capillarity tests and mechanical tests.

3.1 XRD analysis and morphological investigations

The XRD pattern on the as melt is reported in fig. 3a, whilst the diffraction pattern obtained for the scaffold after milling is shown in fig. 3b (950 °C for 3 h) and 3c (1000 °C for 3 h). As it can be observed the as-poured CEL2 is a completely amorphous glass and a broad halo was found. The

thermal treatment carried out to produce the scaffolds induced the nucleation of two crystalline phases, that were identified as combeite ($\text{Na}_4\text{Ca}_4(\text{Si}_6\text{O}_{18})$, JCPDF 01-078-1649) and akemanite ($\text{Ca}_2\text{Mg}(\text{Si}_2\text{O}_7)$, JCPDF 01-077-1149) according to the two T_{XX} found with the thermal analysis [29]. No significant difference was found between the samples sintered at 950°C and 1000°C, since the 2 crystallization temperatures are both below the sintering temperatures.

The results of the sponge impregnation process can be observed in figure 4, 5 and 6, referring to method A, B and C respectively. For what concerns method A, most of the pores are still open after the impregnation process (figure 4a), but the sponge trabeculae are only partially covered by the glass powders (figures 4b and 4c). On the contrary, method B was more effective for the sponge impregnation: some clotted pores can be observed in figure 5a, probably due to an incomplete slurry removal, but the sponge trabeculae were almost uniformly covered by CEL2 powders (figures 5b and 5c). Method C gives the best results, involving a complete and uniform coating of the sponge trabeculae with CEL2 particles (figures 6b and 6c). Some clotted pores are visible (fig. 6a), due to the lack of compressions after the fourth sponge impregnation (table 1).

Figure 7 shows, as an example, the surface and the cross-section of a sintered scaffold obtained with method B. Some clotted pores can be observed, as already noticed in fig. 5 for the impregnated sponge. Figures 8 and 9 show that a high pore interconnection and a very good sintering degree of CEL2 particles was achieved both with method A and method B. The sintering temperature was increased in method B-2 from 950 up to 1000 °C in order to obtain a further improvement of trabeculae densification. Figure 10 shows that an excellent result was achieved, because the trabeculae are well densified (fig. 10a) and it was almost impossible to distinguish the original glass particles (fig. 10b). Similar features were achieved by adopting the method C; the resulting porous structure of the scaffold is showed in fig. 11. It should be noticed that the trabeculae of C-scaffold (fig. 11a) are thicker than the struts of B-2-scaffold (fig. 11b). The same sintering temperature (1000 °C) was used both for method B-2 and C, but in the latter one no sponge compressions were

performed after the fourth impregnation cycle, thus involving a better coating of sponge structure by CEL2 particles.

The structure of the polymeric sponge was substituted by a sintered scaffold with similar texture; the resulting trabecular structure, possessing a highly interconnected network of macropores ranging within 100-600 μm , closely mimicking the natural cancellous bone.

3.2 Porosity analysis

The total porosity was assessed through weight measurement on $1\text{ cm} \times 1\text{ cm} \times 1\text{ cm}$ cubic samples, knowing the CEL2 true density (2.6 g/cm^3). Table 2 reports the so calculated porosity values comparing the results obtained for the different preparation methods. The porosity values obtained for all the prepared samples are well above 50% vol. and thus completely satisfy the requirements for a in-growth material for bone grafting.

The volumetric shrinkage of the samples, calculated testing 5 specimens for each method of scaffold production, is reported in table 3. The data are consistent with the porosity values reported in table 2; in fact, a higher volumetric shrinkage of the scaffold involves a decrease of the pores content. A low standard deviation was found for the samples shrinkage, assessing a good reproducibility of the adopted preparation methods. In addition, it is possible to obtain scaffolds of desired shape and size by carefully tailoring the size of PU sponge, as already reported in fig. 2.

Figure 12 reports the results of capillarity tests. Specifically, fig. 12a shows the sample appearance immediately after the test: the fluid went up through scaffold pores network in about 2 s. In figure 12b the cross-sections of a CEL2 scaffold after the test and of an as-done scaffold are compared. The presence of the serum in the inner part of the scaffold further confirms the high interconnection degree of the porous texture.

Moreover, the scaffolds porosity was quantitatively investigated by means of image analysis carried out on scaffold cross-sections using the Qwin Program of Leica; this technique aims to assess the

pores size distribution and the total pores amount. First, the porosity of different SEM micrographs is highlighted by increasing the black and white contrast; then, a measure frame is selected and the software elaborates the images as binary pictures identifying the dark area as pores. The equivalent pores diameter is evaluated as $2\sqrt{A/\pi}$, where A is the effective area calculated by the software. The acquired data are further processed to obtain two bar charts showing the pores amount and the pores area versus the pores equivalent diameter.

An example of the analysis, referring to method B, is reported in fig. 13; analogous results were obtained for the scaffolds prepared with the other methods.

All the prepared scaffolds are characterized by a bimodal porous structure, in which both micropores (size below 100 μm) and macropores (size within 100-1000 μm) can be identified. The presence of micropores, creating a roughness on scaffold walls, is an important feature because small pores promote proteins and cells adhesion *in vivo* [16,17]. As shown in fig. 13a, the contribution of the micropores was prevalent in terms of pores amount (over 80%).

Macropores over 100 μm are fundamental for a good vascularisation of the implant to allow the blood vessels to reach the inner part of the scaffold [15]. Figure 13b shows that the main contribution to the total pores area (about 80%) was given by pores within 100-1000 μm .

3.3 Mechanical strength tests

Five samples (1 cm \times 1 cm \times 1 cm cubic samples) for each method of scaffold production were tested in compression; the results are reported in table 4.

An example of the stress-strain curve for the CEL2 scaffold is reported in fig. 14. In particular, the curve has a positive slope up to a first peak; then the scaffold begins to crack in the thinner struts at the stress-concentrating sites, causing an apparent stress drop. This is known as “pop-in behaviour” and corresponds to the onset of thin trabeculae cracks propagation. Nevertheless, the scaffold was

still able to bear higher loads, so that the stress rises again; the repetition of this behaviour gave a jagged stress-strain curve while the thin struts cracking occurs. When the maximum stress is reached, the thick struts are fractured and so the curve has a negative slope.

The pore content was the crucial factor affecting the mechanical properties of the scaffolds. The total porosity (table 2), assessed via density measurements, was high for the scaffolds prepared with method A ($68.5 \pm 4.6\%$ vol.), but the mechanical strength was low (1.6 ± 0.5 MPa) with respect to the spongy bone (2-12 MPa) [18]. For the scaffolds prepared with method A-1, the total pore amount ($72.3 \pm 3.3\%$ vol.) and the mechanical strength (1.3 ± 0.4 MPa) were close to the values obtained with method A, thus it was possible to conclude that the drying treatment, adopted before the sintering process, has no significant influence for the scaffold strength.

The scaffolds prepared with method B showed a higher mechanical strength compared to the scaffolds prepared with method A, due to the presence of a lower porosity in the latter ones; as expected, a decrease of the porosity involved an increase of the compressive strength. The strengths of the scaffolds obtained with methods B (3.9 ± 0.4 MPa), B-1 (3.8 ± 0.4 MPa) and B-2 (4.7 ± 0.6 MPa) are comparable to the strength of the cancellous bone (2-12 MPa).

No significant differences, concerning porosity and mechanical strength, were introduced by using the ethylene glycol (EG) in the starting slurry as DCCA slurry (method B-1) and so this additive was not used for methods B-2 and C.

Instead, the increase of sintering temperature from 950 up to 1000 °C intensely influenced the strength of the scaffolds (method B-2) by promoting a higher densification of the struts. Therefore the scaffolds prepared with method C were directly sintered at 1000 °C. A further increase of the compressive strength (5.4 ± 1.5 MPa), consistent with a decrease of the total pore content of the scaffolds ($53.5 \pm 3.7\%$ vol.), was finally reached through this last method.

A very significant improvement in the mechanical strength was attained in comparison with a previous work in which CEL2 scaffolds possessing a strength of 1.0 ± 0.4 MPa were prepared [25]. In particular, the most interesting samples are the ones produced with methods B-2 and C. The

choice of a preparation method, that involves the features of the scaffold in terms of pores content and strength, is related to the specific application of the implant. For general purposes, the best compromise between high porosity and mechanical properties is represented by the scaffolds prepared with method B-2, whereas the method C can be used to fabricate scaffolds requiring specifically high-strength features.

Finally, regarding the values of pores content and mechanical strength reported in tables 2 and 4 respectively, for any series of scaffolds a very low standard deviation was observed, thus assessing the reproducibility of all the proposed methods.

3.4 *In vitro* bioactivity

Figure 15a shows, as an example of *in vitro* bioactivity tests, the surface of a scaffold after 1 week of soaking in SBF. As it can be observed, the scaffold struts are completely covered by globular hydroxyapatite (HAp) agglomerates, whose presence is also confirmed by XRD analysis reported in fig. 15b (JCPDF 01-082-1943).

Besides, as previously assessed [25], CEL2 scaffolds exhibited excellent biological properties when tested with MG-63 cells line (American Type Culture Collection, Rockville, USA). CEL2 scaffold biological behaviour is illustrated, as an example, in fig. 16, where a very good colonisation of the scaffolds by osteoblasts can be observed both after 10 days and 20 days of incubation. The cells appeared strongly adherent on scaffold surface with many protrusions due to their filopodia. MG-63 cells preferentially anchored across the HAp agglomerates (the scaffolds were pre-treated in SBF for 1 week), and exhibited a smooth and flatten morphology indicating that CEL2 scaffolds are an excellent substrate for osteoblasts attachment, spreading and proliferation.

4 Conclusions

In this research work, 3-D bioactive glass-ceramic scaffolds were obtained via the sponge-impregnation method followed by a thermal treatment in order to remove the organic phase and to sinter the inorganic one. A polyurethane open-cells sponge was used as a template. The obtained scaffolds are characterized by a trabecular texture similar to the spongy bone, with open, highly interconnected macropores and a diffused microporosity.

The sponge impregnation parameters and the sintering temperature were successfully optimised in order to obtain scaffolds with a satisfactory degree of porosity and mechanical strength comparable with the trabecular bone (2-12 MPa). Scaffolds functional for general applications, exhibiting a very good compromise between pores content (over 50 %vol.) and strength (over 4 MPa), were prepared. Moreover, scaffolds having a lower porosity degree (over 50 %vol.) and even higher mechanical strength (above 5 MPa) were also produced for high strength bone grafting applications.

Therefore, due to their very good mechanical properties and high bioactivity, CEL2 scaffolds can be suggested as effective implants for bone substitutions.

References

1. J. A. GOULET, L. E. SENUNAS, G. L. DeSILVA and M. L. GREENFIELD, *Clin. Orthop. Rel. Res.* **339** (1997) 76-81.
2. E. M. YOUNGER and M. W. CHAPMAN, *J. Orthop. Trauma.* **3** (1989) 192-195.
3. K. A. HING, F. W. WILSON and T. BUCKLAND, *Spine* **7** (2007) 475-490.
4. C. J. ANKER, S. P. HOLDRIDGE, B. BAIRD, H. COEHN and T. A. DAMRON, *Clin. Orthop. Rel. Res.* **434** (2005) 251-257.
5. B. R. MOED, S. E. WILSON-CARR, J. G. CRAIG and J. T. WATSON, *Clin. Orthop. Rel. Res.* **410** (2003) 303-309.
6. P. HINZ, E. WOLF, G. SCHWESINGER, E. HARTELT and A. EKKERNKAMP, *Orthopedics* **25**(5 suppl) (2002) 597-600.
7. T. YAMAMOTO, T. ONGA, T. MARUI and K. MIZUNO, *J. Bone Joint Surg. Br.* **82** (2000) 1117-1120.
8. K. E. SALYER and C. D. HALL, *Plast. Reconstr. Surg.* **84** (1989) 236-244.
9. G. R. MEADOW, *Orthopedics* **25**(5 suppl) (2002) 579-584.
10. R. MORTERA, B. ONIDA, S. FIORILLI, V. CAUDA, C. VITALE-BROVARONE, F. BAINO, E. VERNÉ and E. GARRONE, *Chem. Eng. J.* **137** (2008) 54-61.
11. R. Z. LEGEROS, S. LIN, R. ROHANIZADEH, D. MIJARES and J. P. LEGEROS, *J. Mater. Sci.:Mater. Med.* **14** (2003) 201-209.
12. Y. ZHANG, H. H. K. XU, S. TAGAKI and L. C. CHOW, *J. Mater. Sci.:Mater. Med.* **17** (2006) 437-445.
13. J. JONES and L. L. HENCH, *Curr. Opin. Solid State Mater. Sci.* **7** (2003) 301-307.
14. C. VITALE-BROVARONE, E. VERNÉ and P. APPENDINO, *J. Mater. Sci.:Mater. Med.* **17** (2006) 1069-1078.

15. P. N. DE AZA, Z. B. LUKLINSKA, C. SANTOS, F. GUITIAN and S. DE AZA, *Biomat.* **24** (2003) 1437-1445.
16. D. ROKUSEK, C. DAVITT, A. BANDYOPADHYAY, S. BOSE and H. L. HOSICK, *J Biomed. Res.* **75** (2005) 588-594.
17. Z. SCHWARTS and B. D. BOYAN, *J. Cell. Biochem.* **56** (1994) 340-347.
18. J. D. THOMPSON and L. L. HENCH, *J. Eng. in Med.* **212** (1998) 127-136.
19. Q. Z. CHEN, I. D. THOMPSON and A. R. BECCACCINI, *Biomat.* **27** (2006) 2414-2425.
20. X. MIAO, G. LIM, K. H. LOH and A. R. BOCCACCINI, *Mater. Proc. Prop. Perf. (MP3)* **3** (2004) 319-324.
21. L. L. HENCH, *J. Mater. Biomed. Res.* **41** (1998) 511-518.
22. T. W. BAUER and S. T. SMITH, *Clin. Orthop.* **395** (2002) 11-22.
23. J. R. JONES, L. M. EHRENFRIED and L. L. HENCH, *Biomat.* **27** (2006) 964-973.
24. N. L. PORTER, R. M. PILLIAR and M. D. GRYNPAS, *J. Biomed. Mater. Res.* **56** (2001) 504-515.
25. C. VITALE-BROVARONE, E. VERNÉ, L. ROBIGLIO, P. APPENDINO, F. BASSI, G. MARTINASSO, G. MUZIO and R. CANUTO, *Acta Biomater.* **3** (2007) 199-208.
26. C. VITALE-BROVARONE, M. MIOLA, C. BALAGNA and E. VERNÉ, *Chem. Eng. J.* **137** (2008) 129-136.
27. O. LYCKFELDT and J. M. FERREIRA, *J. Eur. Ceram. Soc.* **18** (1998) 131-140.
28. C. VITALE-BROVARONE, S. DI NUNZIO, O. BRETCANU and E. VERNÉ, *J. Mater. Sci.:Mater. Med.* **15** (2004) 209-217.
29. C. VITALE-BROVARONE, E. VERNÉ, L. ROBIGLIO, G. MARTINASSO, R. CANUTO and G. MUZIO, *J. Mater. Sci.:Mater. Med.* **19** (2008) 471-478.
30. N. UCHIDA, N. ISHIYAMA, Z. KATO and K. UEMATSU, *J. Coatings Tec. Res.* **29** (1994) 5188-5192.
31. T. KOKUBO and H. TAKADAMA, *Biomat.* **27** (2006) 2907-2915.

Figure legends

Fig. 1 Polyurethane sponge structure.

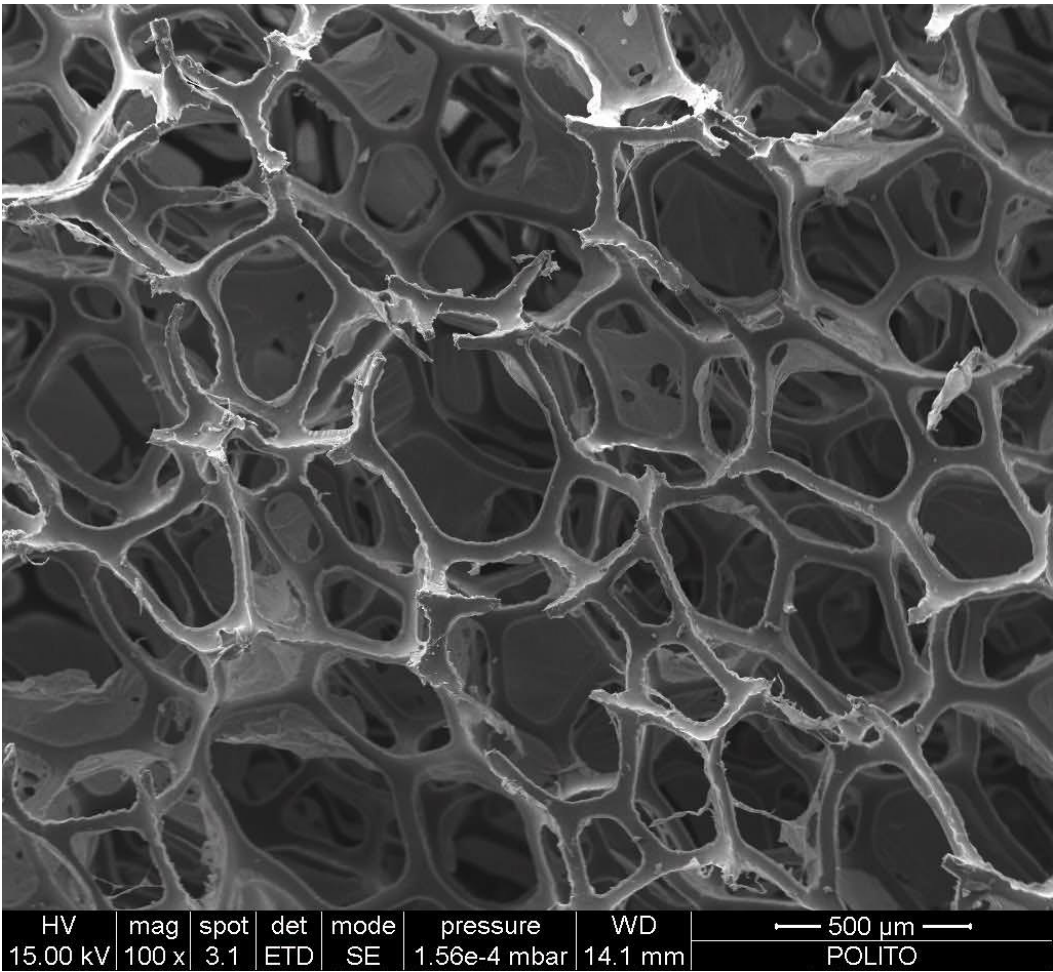


Fig. 2 CEL2 scaffolds: (a) cubic samples and (b) and prism-shaped samples.

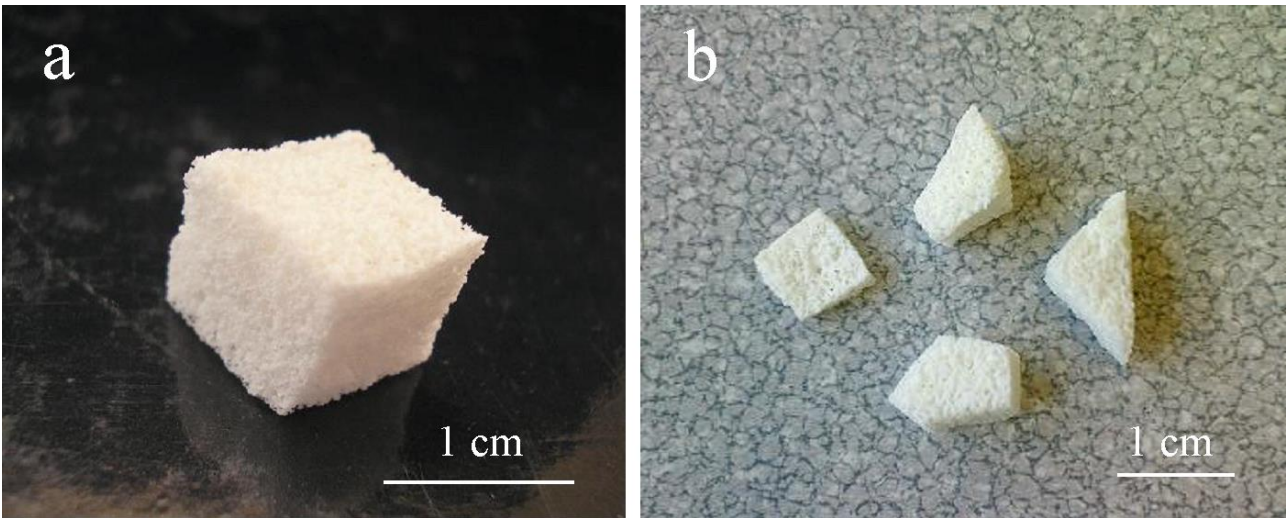


Fig. 3 Diffraction patterns of (a) as-poured CEL2 and of CEL2 scaffold obtained after thermal treatment at (b) 950 °C or (c) 1000 °C for 3 h.

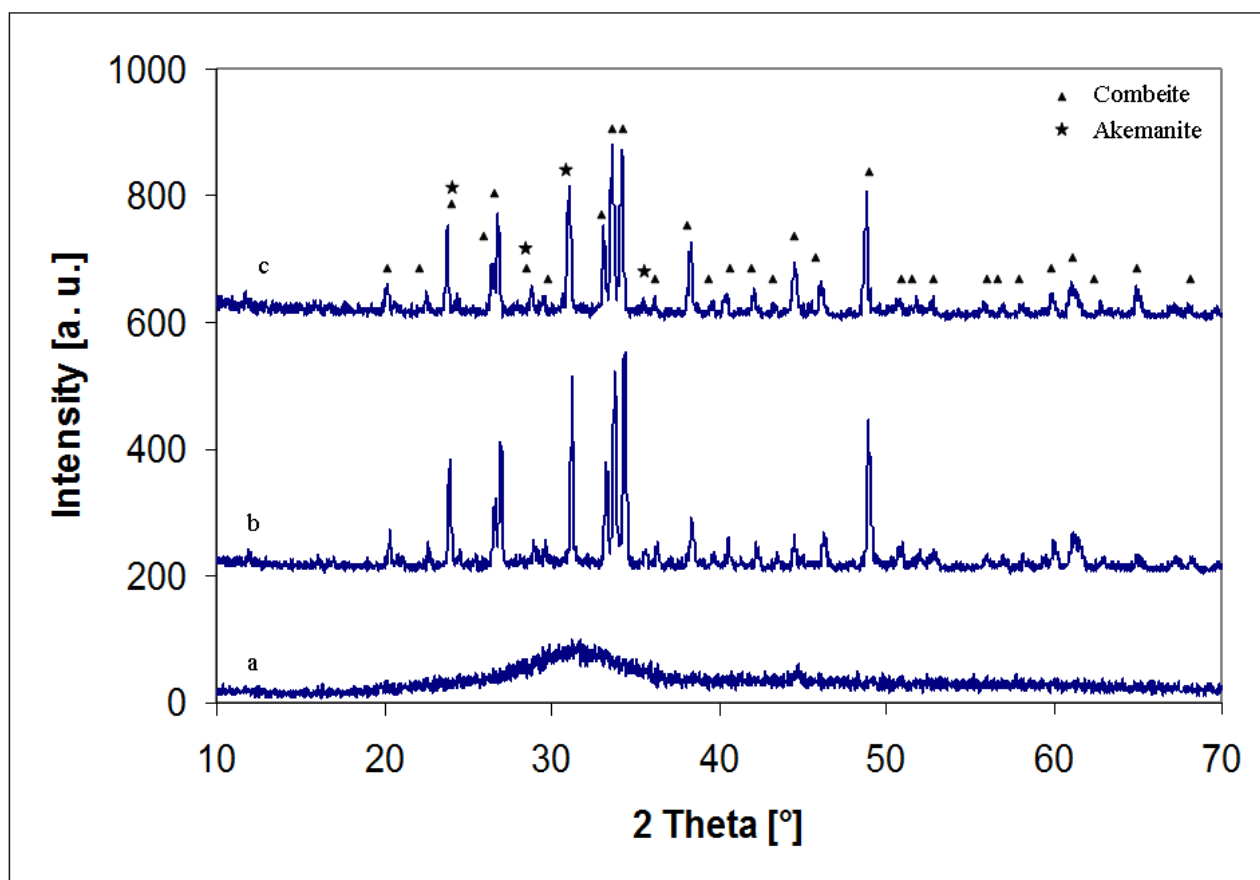


Fig. 4 Micrographs of the sponge impregnated with method A at different magnifications.

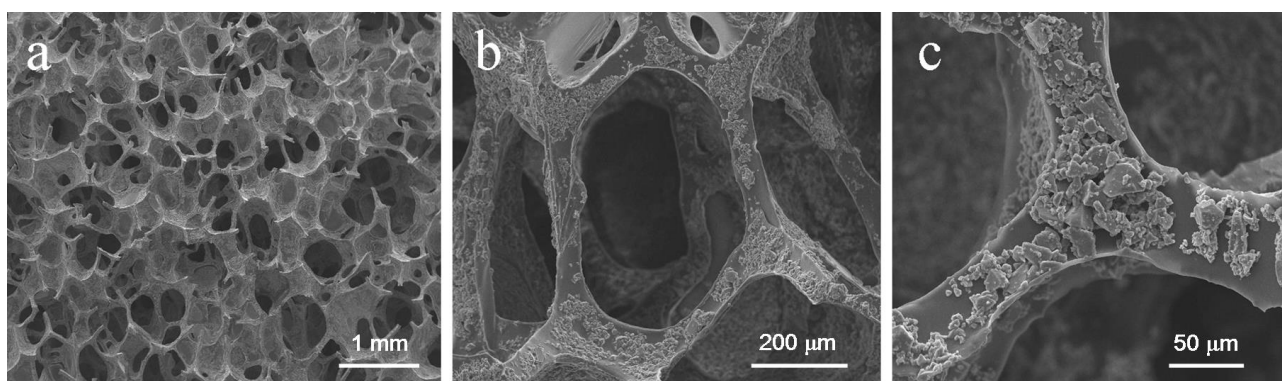


Fig. 5 Micrographs of the sponge impregnated with method B at different magnifications.

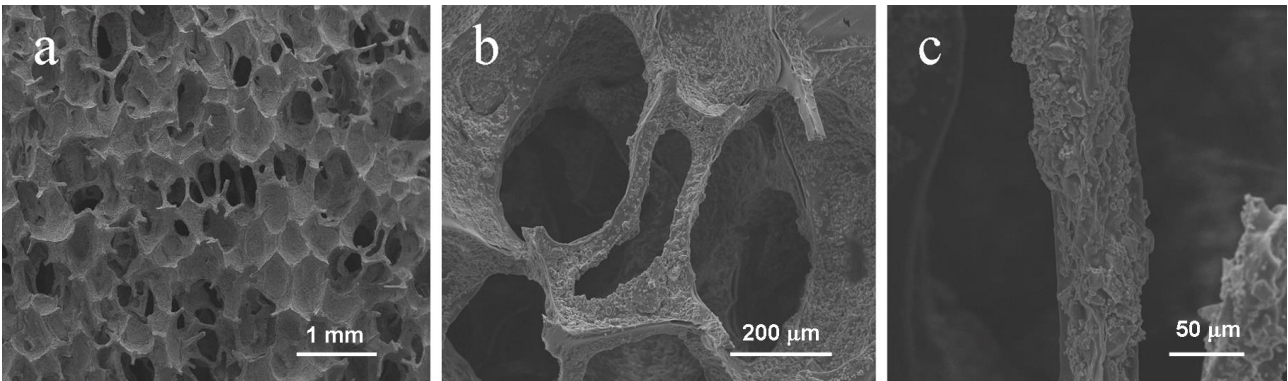


Fig. 6 Micrographs of the sponge impregnated with method C at different magnifications.

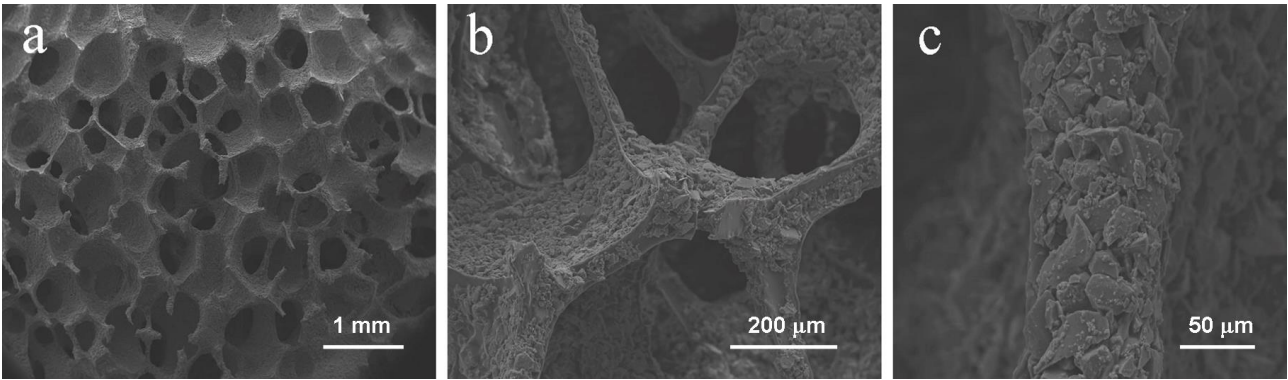


Fig. 7 Micrographs of CEL2 scaffold prepared with method B: (a) surface and (b) cross-section.

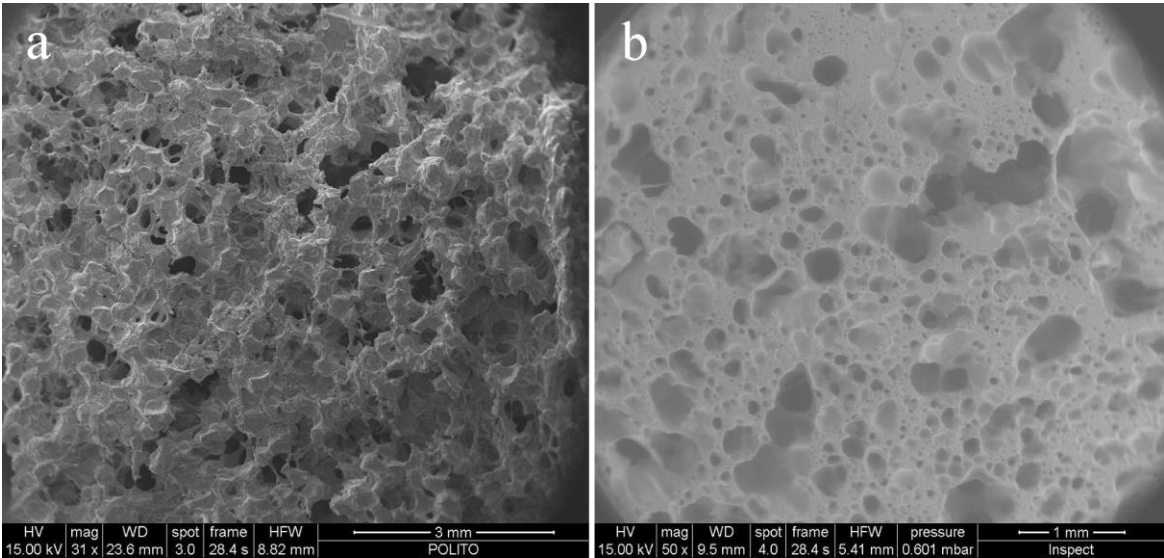


Fig. 8 Micrographs showing the high pores interconnection of a scaffold obtained with method A.

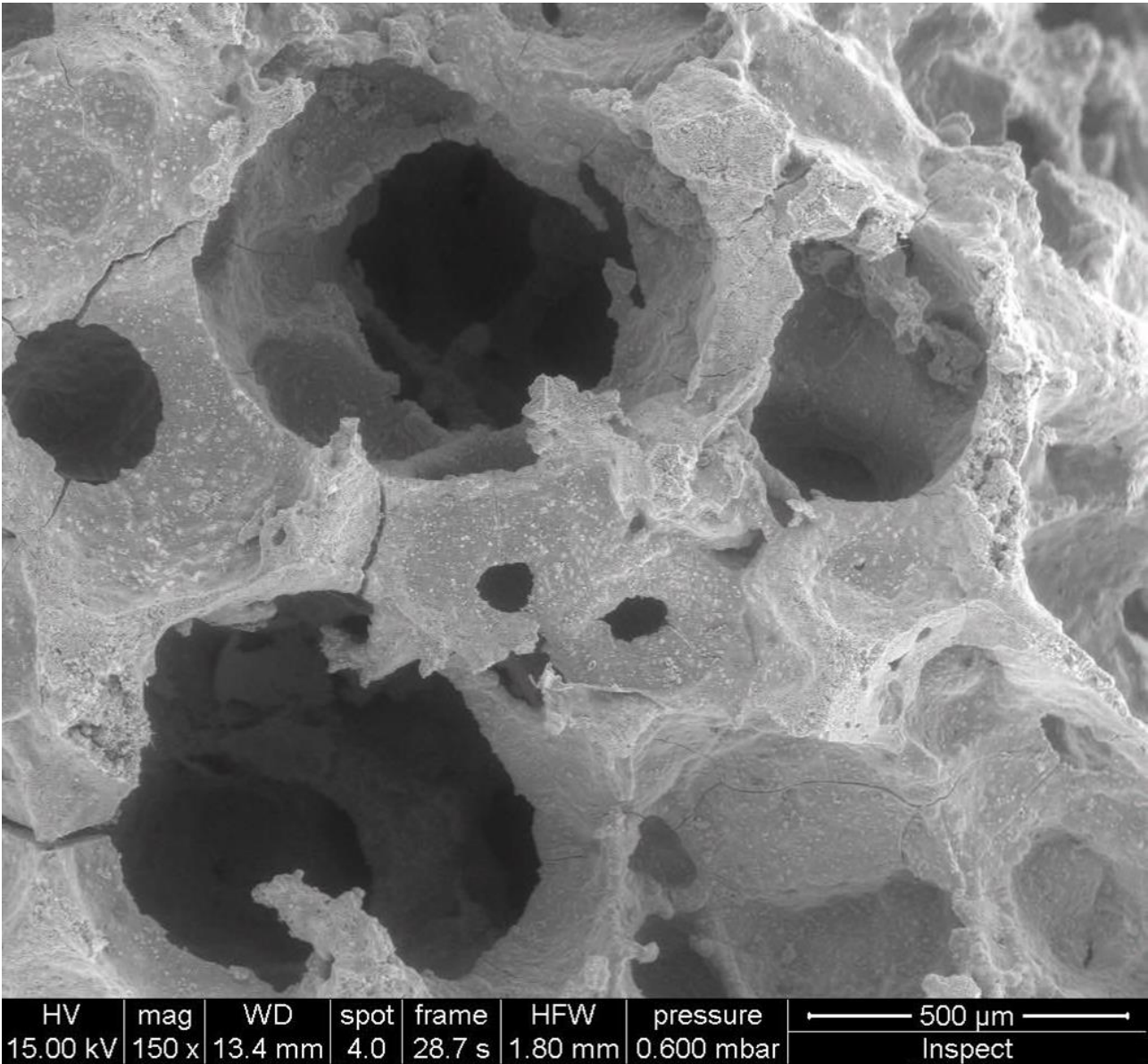
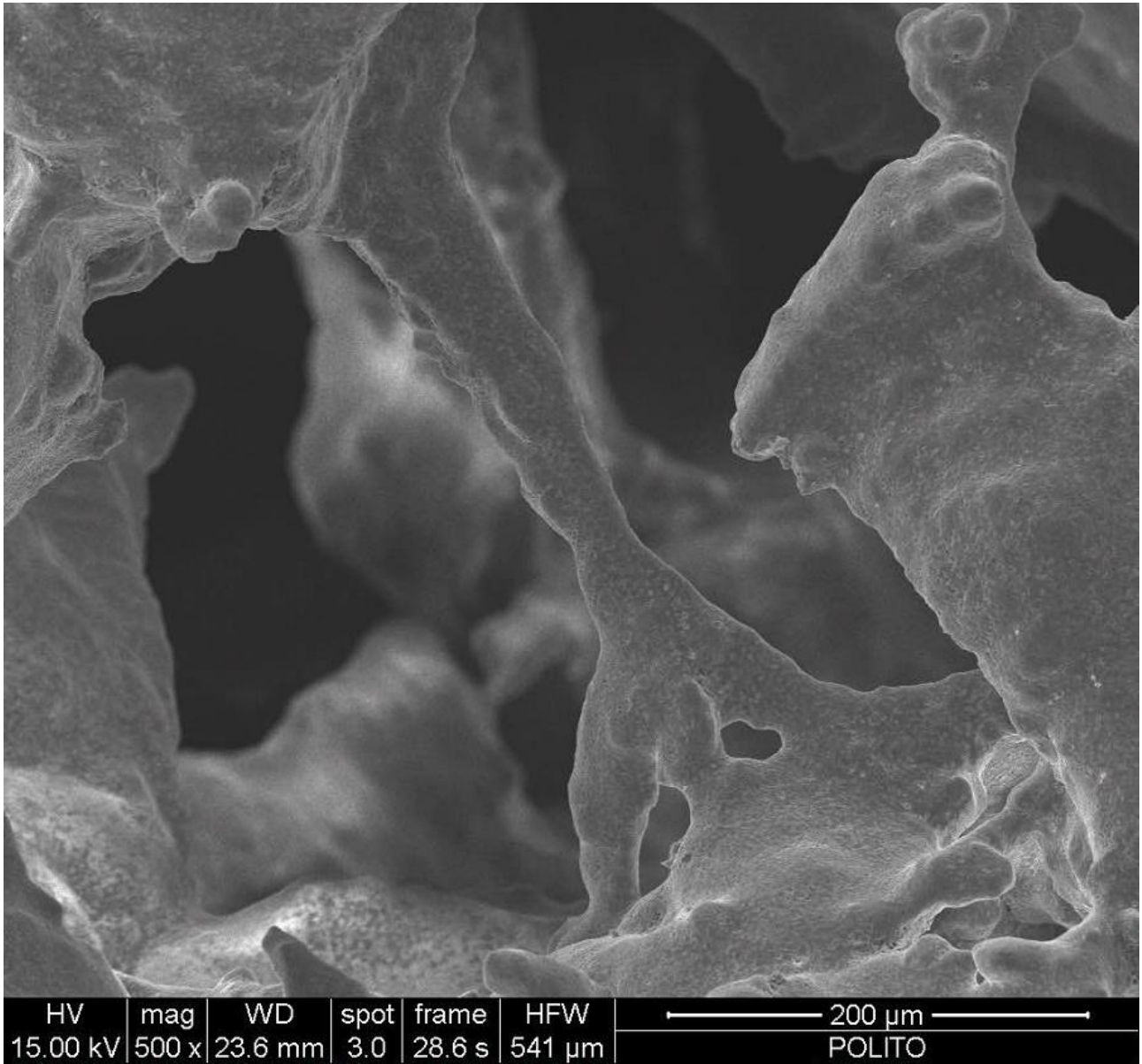


Fig. 9 Well-sintered trabeculae of CEL2 scaffold prepared with method B.



HV	mag	WD	spot	frame	HFW
15.00 kV	500 x	23.6 mm	3.0	28.6 s	541 μm

200 μm
POLITO

Fig. 10 Micrographs of (a) macropores and (b) their well-sintered struts (b) in a scaffold prepared with method B-2.

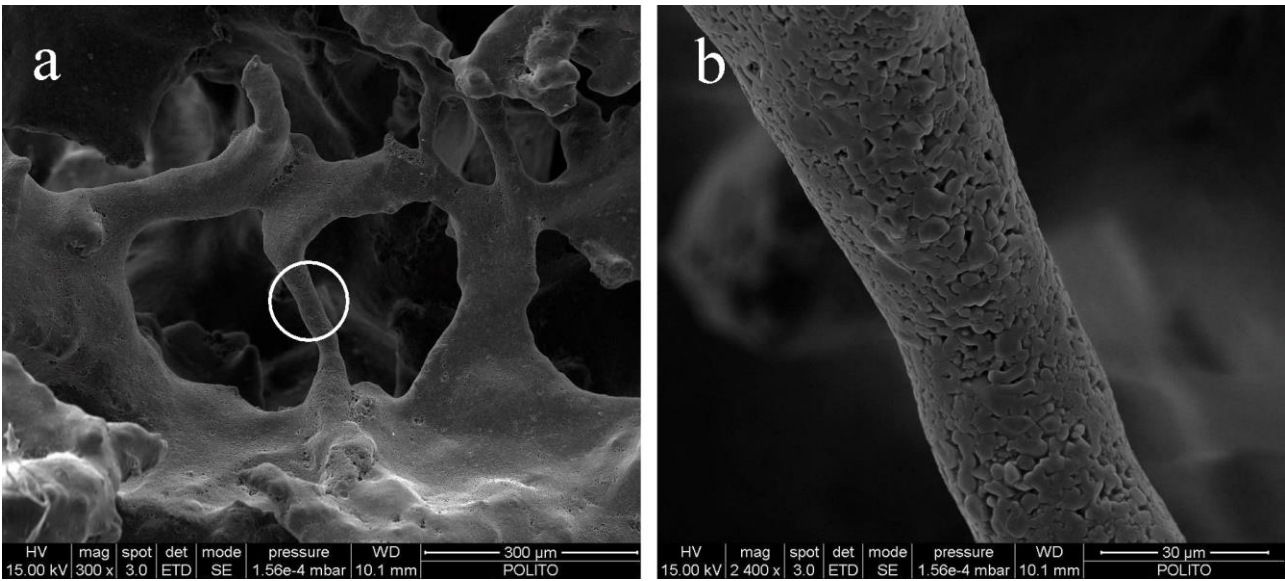


Fig. 11 Micrographs of the scaffold prepared with method C: (a) macropores with their struts and (b) particular of a trabecula.

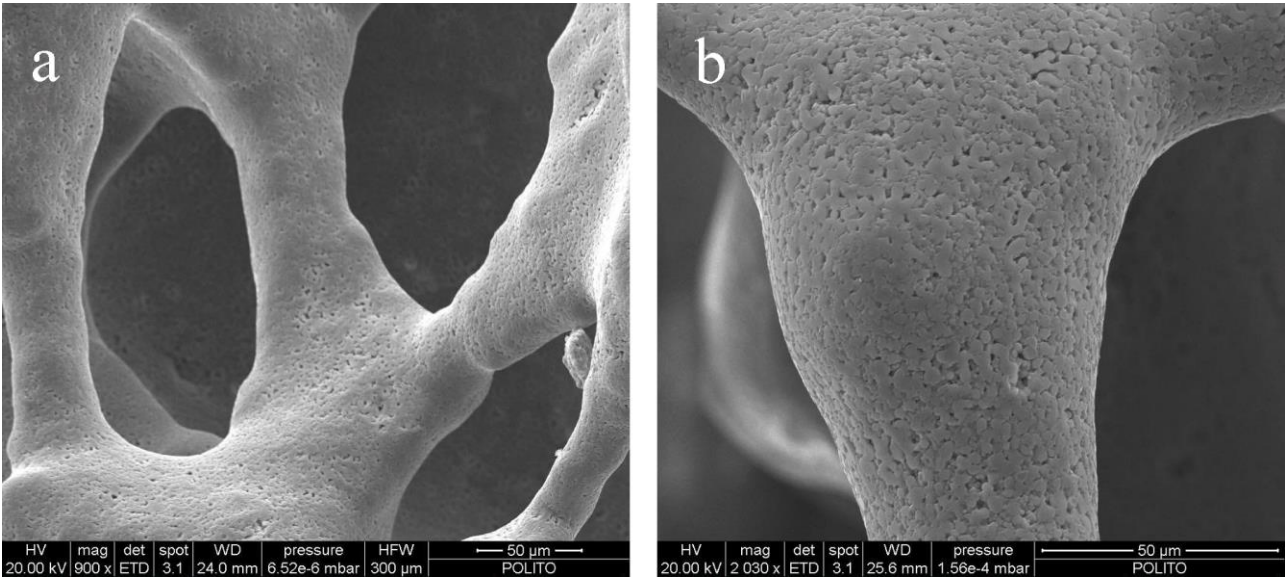


Fig. 12 (a) Capillarity test performed on CEL2 scaffold and (b) comparison between the cross-sections of a sample after the test and an as-done scaffold.

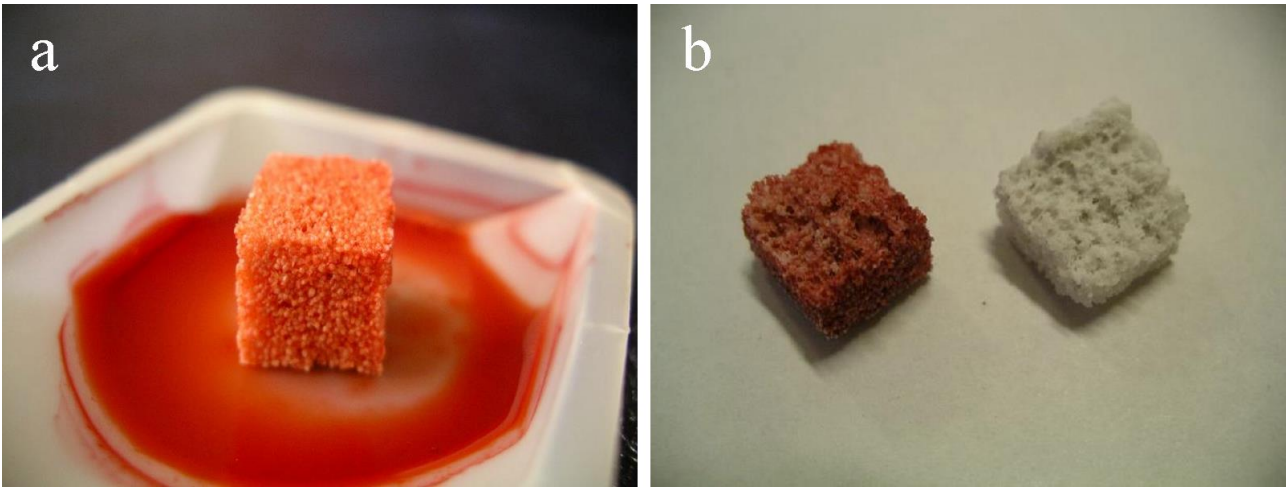


Fig. 13 Image analysis results: (a) pores amount and (b) pores area.

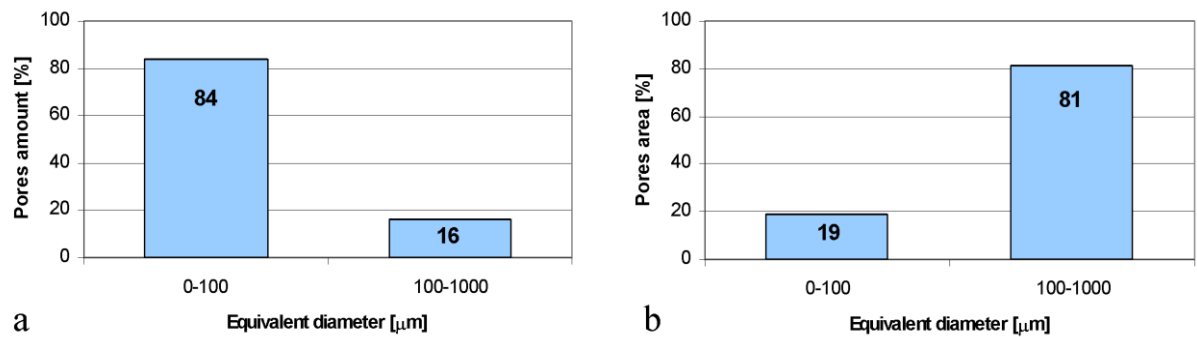


Fig. 14 Typical compressive CEL2-scaffold stress-strain curve.

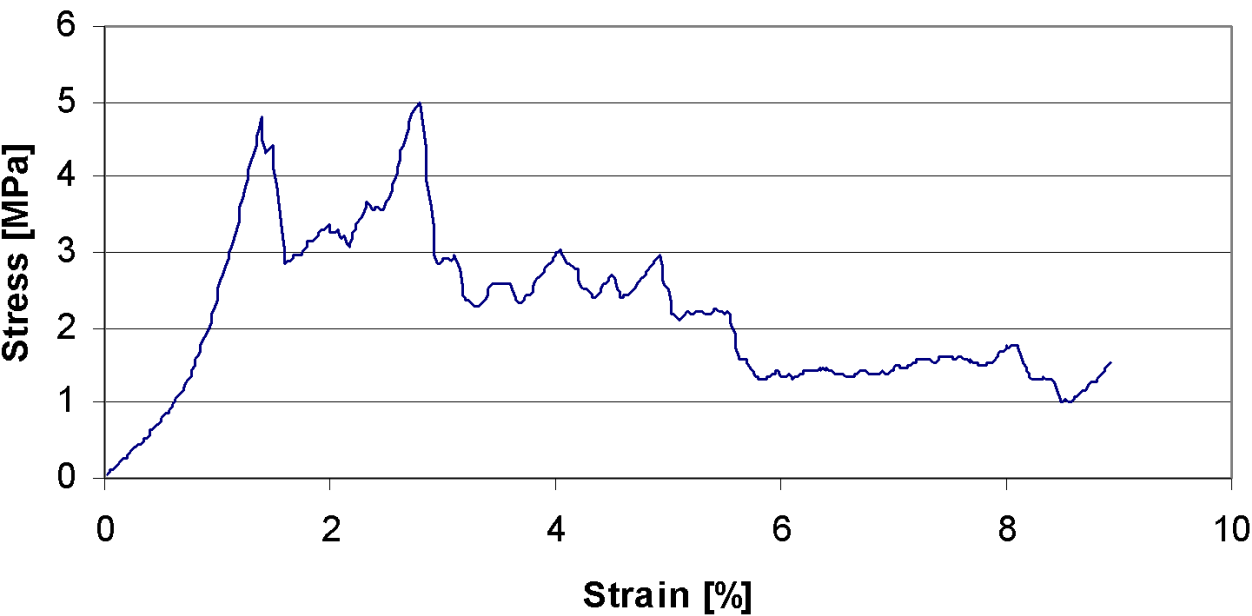


Fig. 15 *In vitro* tests: (a) HAp agglomerates on scaffold surface after 1 week in SBF and (b) corresponding diffraction pattern.

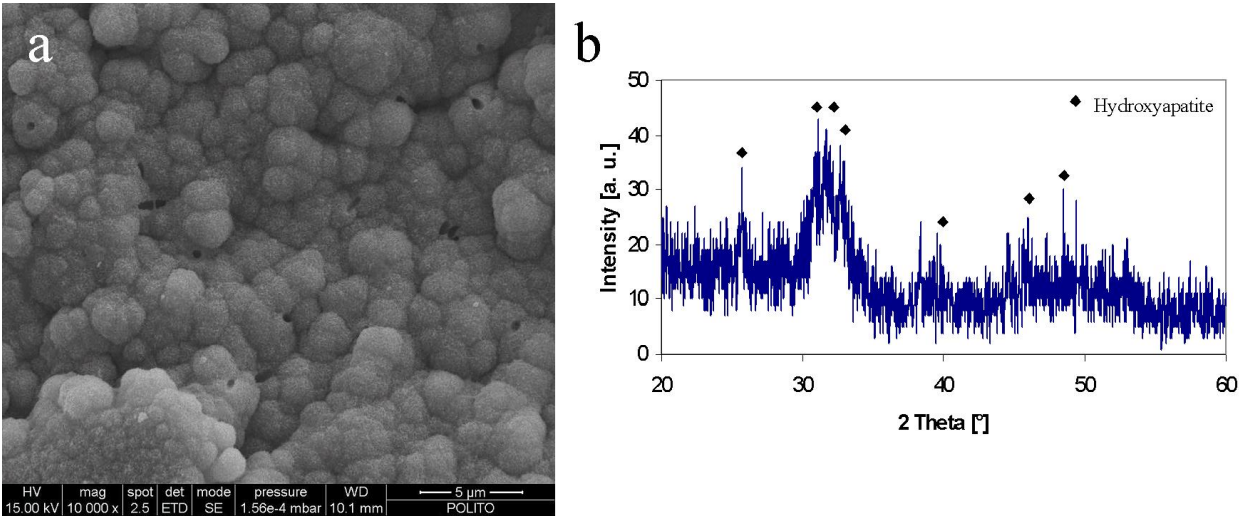
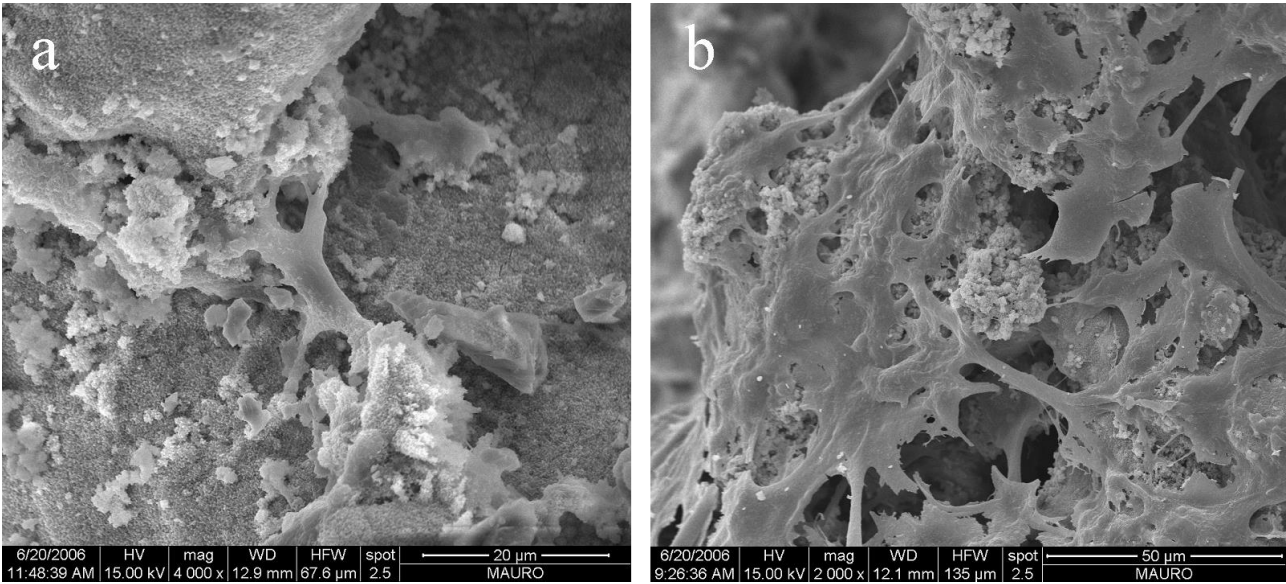


Fig. 16 MG-63 cells on CEL2 scaffold after (a) 10 days and (b) 20 days of culture.



Tables

Table 1 Preparation methods of CEL2 scaffolds.

Preparation method	Cycles of infiltration/compression	Additives	Drying	Thermal treatment
A	Cycle: 1 impregnation followed by 3 compressions of 60%; the cycle is repeated for 3 times.	No	3 h at room temperature	950 °C for 3 h
A-1	Such as A	No	3 h at room temperature + 80 °C for 2h + 600 °C for 2 h	950 °C for 3 h
B	Cycle: 1 impregnation followed by 3 compressions of 60%; the cycle is repeated for 3 times and then another impregnation is carried out with a compression of 33%.	No	3 h at room temperature	950 °C for 3 h
B-1	Such as B	Ethylene glycol (10% wt.)	Such as B	950 °C for 3 h
B-2	Such as B	No	Such as B	1000 °C for 3 h
C	Cycle: 1 impregnation followed by 3 compressions of 60%; the cycle is repeated for 3 times and then another impregnation is carried out without compression.	No	Such as B	1000 °C for 3 h

Table 2 Total porosity obtained via density measurements.

Impregnation method	Total porosity (% vol.)
Method A	68.5 ± 4.6
Method A-1	72.3 ± 3.3
Method B	59.4 ± 2.2
Method B-1	55.8 ± 2.2
Method B-2	62.1 ± 1.5
Method C	53.5 ± 3.7

Table 3 Scaffolds volumetric shrinkage.

Impregnation method	Volume shrinkage (%)
Method A	65.2 ± 4.1
Method B	65.2 ± 1.3
Method C	69.9 ± 3.9

Table 4 Compressive strength of the scaffolds (5 samples tested for each preparation method).

Impregnation method	Compressive strength [MPa]
Method A	1.6 ± 0.5
Method A-1	1.3 ± 0.4
Method B	3.9 ± 0.4
Method B-1	3.8 ± 0.4
Method B-2	4.7 ± 0.6
Method C	5.4 ± 1.5